Design and Validation of a Light Vehicle Tubular Space Frame Chassis

Poula kamel, George A. Fayek, Ibrahim Gafar, Ahmed Saad, Helwan University

---

Abstract

This work presents the design of an SAE BAJA space frame based on static finite element analysis. The design of such an off-road vehicle is intended to achieve extreme performance objectives in terms of safety, durability, rigidity, and reliability. First, the frame structural members are selected according to BAJA rules, and it is also constrained by the material availability in the market. Then, a comparison set based on von-misses stress criteria between analytical and three numerical models is constructed. Consequently, the one-dimensional beam element mesh is found to be more efficient regarding computational time and accuracy of the results. However, the engine-frame fixation plate is modeled using two-dimensional elements due to the plate geometry. Secondly, the 3D model of the frame is constructed using SolidWorks software, and the simulation of various loading scenarios including inertial, impact, and frame torsional rigidity tests are implemented using Static Structural Analysis System. Several vehicle parameters are utilized to simulate road-vehicle interaction. Longitudinal and lateral vehicle load transfer as a result of powertrain acceleration, braking deceleration, road grade, and rotational acceleration are considered in the inertial loading tests. Moreover, front, rear, side-impact, and rollover tests are conducted using an equivalent static system to model the possible crash scenarios for the vehicle frame. Furthermore, the torsional stiffness of the vehicle structure is obtained to ensure a safe frame twisting limit resulting from road irregularities. Finally, the simulation results indicate that the proposed vehicle frame can be operated safely through the expected road conditions. Therefore, the developing of the vehicle frame through the manufacturing process can be executed.

Introduction

SAE BAJA is an intercollegiate competition in which many engineering teams contest to achieve certain requirements and performance for an off-road vehicle. These requirements include clear rules that attain fair competitive levels and ensure vehicle driver safety. However, a trade-off between the vehicle frame rigidity and weight must be considered. Since engine capacity is pre-determined by the rules [1], the vehicle frame weight represents a crucial role in the overall vehicle performance.

Many research studies discussed the key factors of the design, simulation, and implementation of the SAE BAJA vehicle frame as in [2], and [3]. Most of these studies discuss the competition's main concern, which is the safety of the vehicle driver as in [4], [5], and [6]. Weight reduction of the frame design is also one of the most important design considerations and could be achieved through many strategies such as minimizing secondary members, and frame design optimization [7], and [8]. Moreover, A modification for Structural rigidity enhancement is analyzed in [9] by using additional strengthening gussets at the critical frame locations where high stresses are detected. Nevertheless, most studies don't focus on meshing quality as a parameter that affects the finite element analysis (FEA) process [10].

In this work, various element criteria are applied to a simple meshed model representing the geometry of the frame members. This technique is used to validate the output results with the analytical values to select the optimal element criteria for frame meshing. Furthermore, the design of the vehicle frame is simulated using ANSYS software in terms of inertial, impact, and frame torsional stiffness simulations to ensure that the vehicle frame can work safely under the predicted off-road conditions.

Frame Design and Validation

Frame Design Considerations

Off-road vehicles are intended to be superior regarding frame strength and torsional rigidity due to their operation in extreme conditions. In the SAE BAJA competition, many rules that are related to safety are a must in terms of min. requirements for outside members' diameters, min. wall thickness, min. carbon content for the utilized material. Moreover, suspension fixation geometry, driver ergonomics, powertrain system fixation, and accessibility are also considered.

Material Selection and Frame Members Cross Sections

Due to the restrictions of SAE BAJA rules concerning the frame material and the availability in the local market, few options are found to be eligible for selection. The selected material properties are shown in Table 1. The utilized frame cross sections for primary and secondary members are obtained in

Table 2.

Table 1 ASTM A-106 Grade. B *Material properties.*

Parameter	Value	Unit
Density	7850	kg/m3
Young's modulus	200	GPa
Poisson ratio	0.3	-
Shear modulus	76.9	GPa
Tensile yield strength	326	MPa
Tensile ultimate strength	517	MPa

Table 2 The primary & secondary member cross-section.

Parameter	Outer Diameter (mm)	Thickness(mm)
Primary	42.164	1.651
Secondary	26.67	2.67

Primary and Secondary Members Validation

The primary and secondary members are validated to ensure the methodology used to simulate the loading scenarios on the frame structure. As depicted in Figure 1, a simple problem is introduced in SolidWorks in which a vertical force of 100 N is acting on the edge of the 1000 mm primary member. This member is connected to another member at a distance from fixed support of 1000 mm.

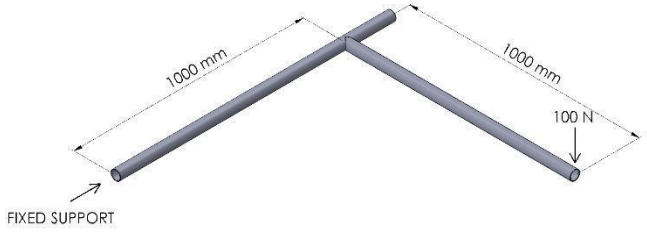

Figure 1 The primary member validation.

The bending stress σ, shear stress due to torque τ, and von-mises stress $\sigma_{Von-Mises}$ are obtained as follows [11]:

$$\sigma = \frac{M * y}{I} \qquad (1)$$

$$\tau = \frac{T * r}{J} \qquad (2)$$

$$\sigma_{Von-Mises} = \sqrt{\sigma^2 + 3\tau^2} \qquad (3)$$

Where I is the second moment of inertia, M is the bending moment, and y $(y = r)$ is the max. distance from the neutral axis, J is the polar moment of area, and T is the torque. The primary and secondary member parameters utilized in the analysis are shown in Table 3 and Table 4. The analytical values obtained from Equations *(1), (2),* and *(3)* are compared to the validated values produced from the modeling process in the Ansys workbench using FEA in 1D beam element, 2D, and 3D mesh types. The resulting stress values are illustrated in Table 5 and Table 6. Also, the error in von-misses stress is obtained from Equation *(4)* as the difference between the analytical value and the value of every mesh type divided by the analytical value as follows [12]:

$$error\ \% = \Delta x / x \qquad (4)$$

Where Δx is the difference between the analytical value and the value of every mesh, and x is the analytical value.

Table 3 The primary member parameters.

Parameter	Value	Unit
M	100*103	N.mm
T	100*103	N.mm
y	21.082	mm
J	86365.61	mm4
I	43182.2	mm4

Table 4 The secondary member parameters.

Parameter	Value	Unit
M	$100*10^3$	N.mm
T	$100*10^3$	N.mm
y	13.335	mm
J	29347.87	mm^4
I	14673.94	mm^4

Table 5 The comparison of the primary member meshing type and size.

	Analytical	3D Mesh	2D Mesh	1D Mesh
Element size (mm)	—	5	5	5
No. of nodes	—	114747	11531	881
σ	48.82	—	—	48.92

τ	24.41	—	—	24.41
$\sigma_{Von-Mises}$	64.58	66.355	65.599	65.23
Error	0%	2.7%	1.6%	1%

Table 6 The comparison of the secondary member meshing type and size.

	Analytical	**3D Mesh**	**2D Mesh**	**1D Mesh**
Element size (mm)	—	5	5	5
No. of nodes	—	70317	6582	881
σ	90.88	—	—	91.06
τ	45.44	—	—	45.44
$\sigma_{Von-Mises}$	120.22	121.59	113.47	120.36
Error	0%	1.1%	5.6%	0.1%

Based on the results shown in Table 5, and Table 6, it's clear that the 1D beam element mesh type in both primary and secondary members is the optimum type in terms of minimum error and computational effort. Hence, the vehicle frame is meshed using a 1D beam element type.

Results and discussion

Inertial Loadings Results

Acceleration while climbing a hill scenario

Various kinds of loadings, inertial, and impact are simulated to develop and validate the vehicle frame design. Inertial loadings are represented in longitudinal and lateral load transfers. Longitudinal load transfers are due to acceleration and braking while lateral load transfer is due to cornering. Additionally, load transfer induced by maximum inclination is considered in every inertial scenario. The fixations for the inertial scenarios are represented in Figure 2 where each fixation point is hinged about the y-axis. In the 1st inertial loading scenario, the vehicle accelerates with the maximum acceleration of the powertrain system and ascends a grade of 25°, causing longitudinal load transfer according to Equation *(5)*. Boundary conditions are applied to the structure as shown in Figure 3 and the weight transfer is expressed by[13]:

$$W_r = \frac{W l_1 cos\,\theta_s + \frac{haW}{g} + Whsin\,\theta_s}{L} \qquad (5)$$

Where W_r is the vehicle weight on the rear axle, W_f is the vehicle weight on the front axle, W is the total vehicle weight, l_1 is the distance from the center of the front axle to the vehicle C.G position, θ_s is the road inclination angle, h is the vehicle C.G height, a is the vehicle acceleration, and L is the vehicle wheelbase.

Acceleration while climbing a hill results

Results show maximum bending stress of 74.54 MPa in the longitudinal members joining the engine and transmission fixation points as expected due to the applied powertrain system torque about the negative Y direction as shown in Figure 4. Consequently, this applied bending moment due to the powertrain system is transmitted to the short lateral members joining the two longitudinal members as a torsional moment with a maximum absolute value of 35.6 N.m as shown in Figure 5. As a result, the maximum torsional shear stress is 16.18 MPa as obtained from Equation *(2)*. Moreover, as the plate welded to the structural members is modeled with shell elements, direct von-mises stress is generated with a maximum value of 125.71 MPa as illustrated in Figure 6. This hotspot in the plate represents a stress concentration produced from a geometry change in the intersection between the plate and the longitudinal frame member. Regarding the previous results, the maximum von-mises stress of 126.95 MPa is captured and recorded in the portions of the frame members subjected to the maximum bending and torsional stresses and intersecting with the engine fixation plate at its maximum von-mises stress as shown in Figure 7. Furthermore, a safety factor of 2.57 can be calculated from Equation *(6)*. Finally, as depicted in Figure 8, the engine plate deformed with 0.4 mm of a maximum absolute total deformation at its far end as a result of the applied powertrain system torque. The directional deformation plot in Figure 9 ensures that the 0.4 mm deformation occurs in the negative Z direction.

$$F.O.S. = \frac{\sigma_{von-Mises}}{\sigma_{yield}} \qquad (6)$$

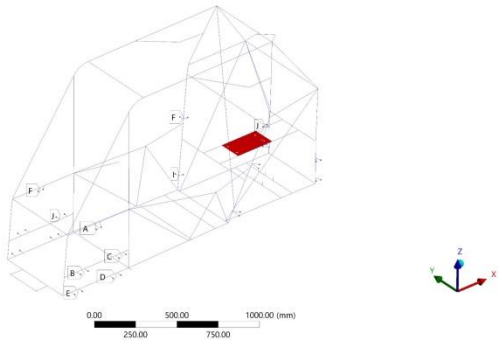

Figure 2 Inertial scenarios fixations

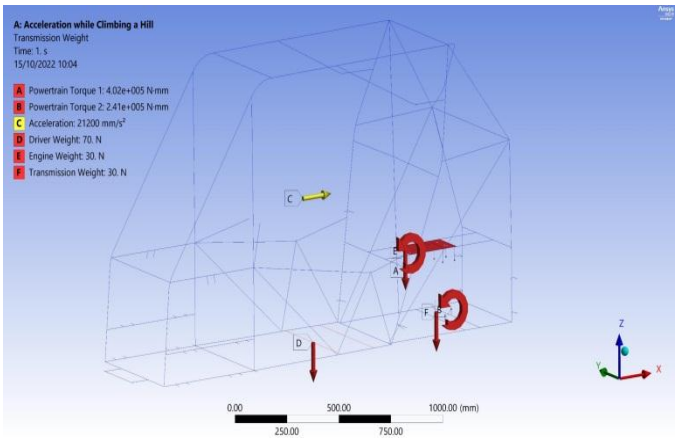

Figure 3 Acceleration while climbing a hill loadings.

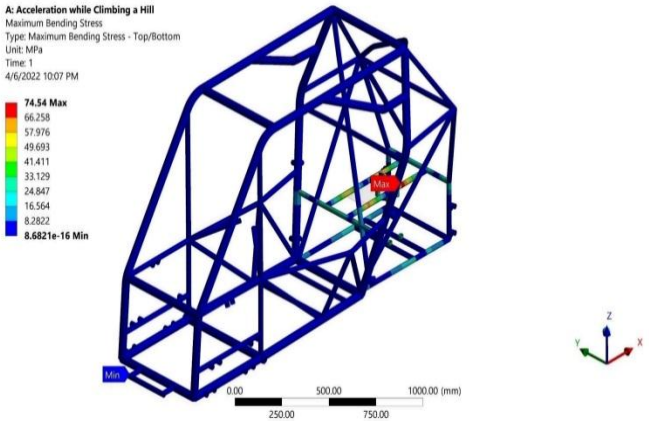

Figure 4 acceleration while climbing a hill beam elements bending stress.

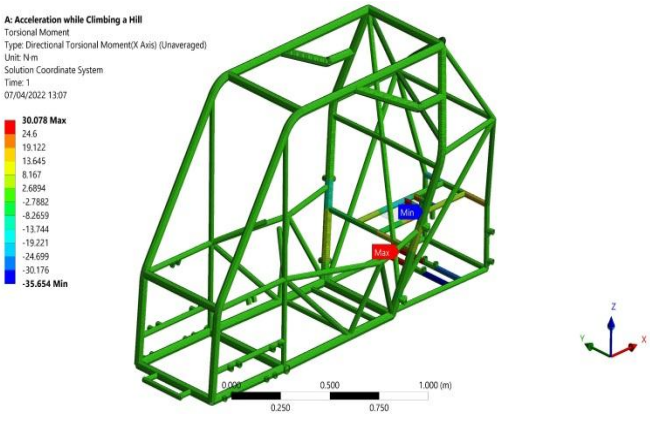

Figure 5 acceleration while climbing a hill torsional moment.

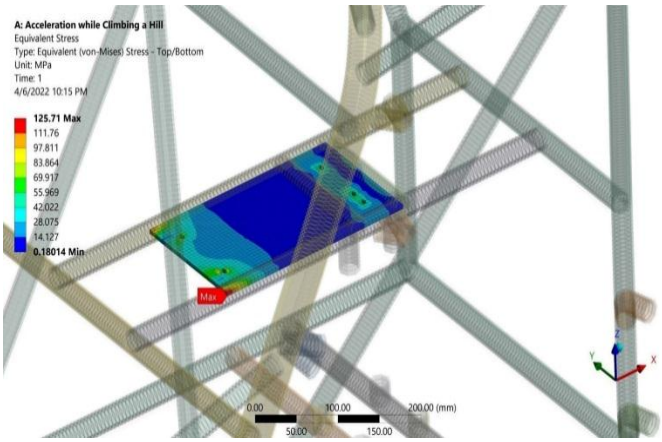

Figure 6 acceleration while climbing a hill shell elements von-mises stress.

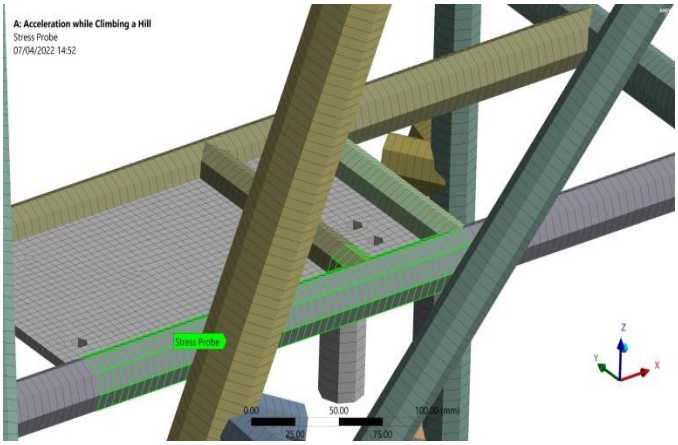

Figure 7 acceleration while climbing a hill beam elements von-mises stress probe.

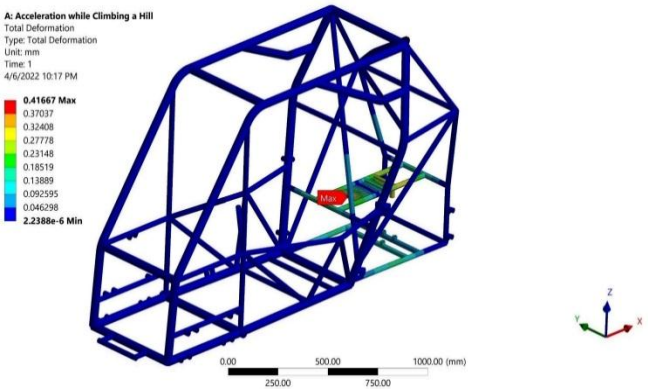

Figure 8 acceleration while climbing a hill total deformation.

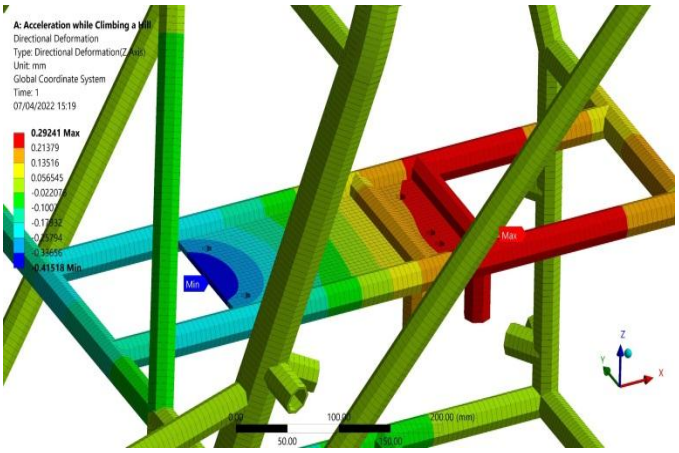

Figure 9 acceleration while climbing a hill directional deformation detailed view.

Deceleration and cornering while descending a hill scenario

The longitudinal load transfer in the 2nd scenario is generated due to the braking action and descending a grade of 25° as represented in Equation *(7)*, while the lateral load transfer is due to a constant angular velocity with a minimum turning radius of 4 meters causing roll moment. The scenario boundary conditions are shown in Figure 10. the weight transfer is expressed by[13]:

$$W_f = \frac{Wl_2 cos\,\theta_s + \frac{haW}{g} + Whsin\,\theta_s}{L} \qquad (7)$$

Where l_2 is the distance from the center of the rear axle to the vehicle C.G position.

Deceleration and cornering while descending a hill results

A bending stress of 10.9 MPa is induced in the far rear vertical members as shown in Figure 11 and a maximum torsional moment of 5.92 N.m occurs in the far lower suspension fixation points as shown in Figure 12. Originally, most of the powertrain system and the driver weights are loaded on the rear axle. Thus, the vertical weight on the rear axle decreased as a result of the longitudinal load transfer between the two axles. Finally, maximum total deformation of 0.017 mm resulted in the rear end of the structure as shown in Figure 13.

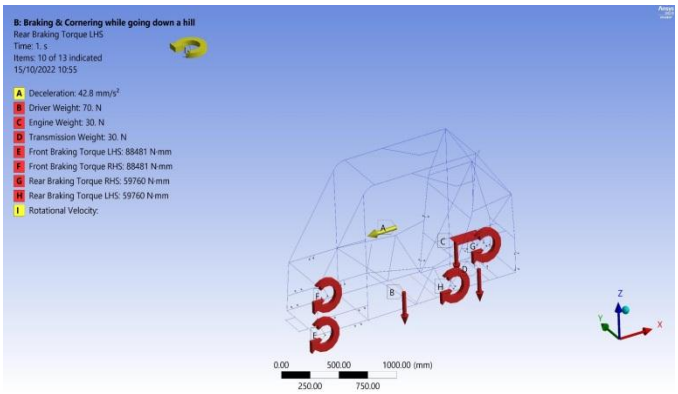

Figure 10 braking loadings.

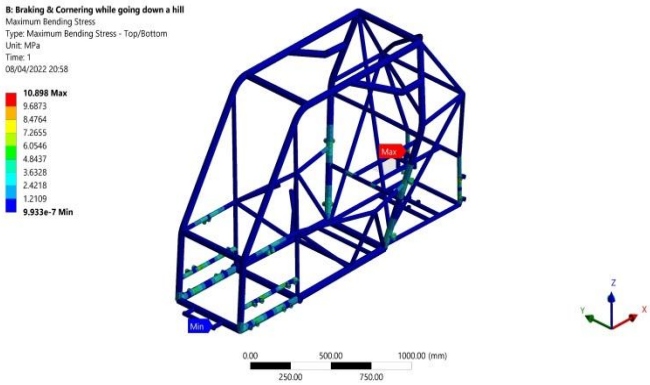

Figure 11 braking bending stress.

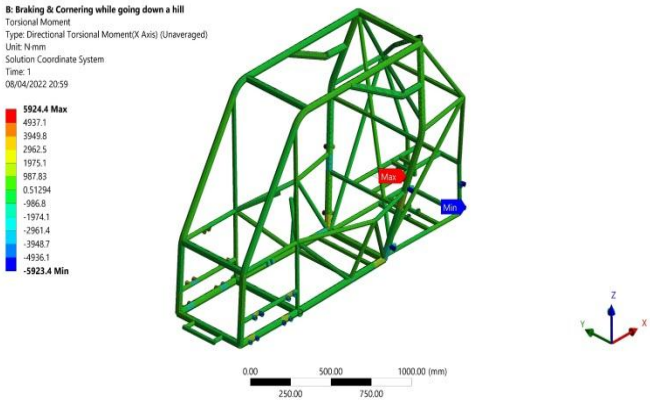

Figure 12 braking torsional moment.

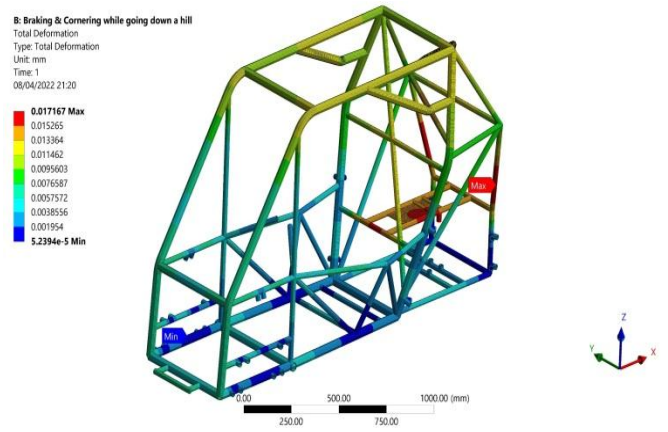

Figure 13 Braking total deformation.

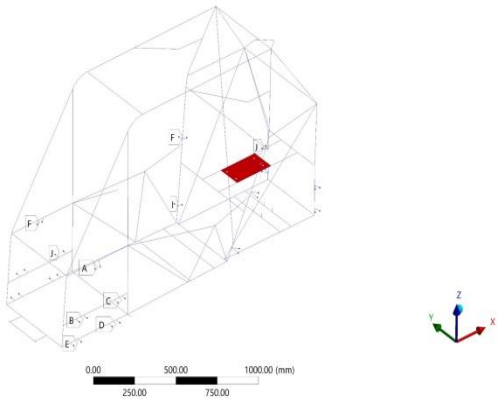

Figure 14 impact scenarios fixations.

Impact loading

Front Impact Loading Scenario

The Static Structural Analysis System in ANSYS workbench is used to simulate impact loadings using the appropriate static force representing the effect of the dynamic event. Generally, the fixations for all impact scenarios are represented in Figure 14 where all of the suspension points' degrees of freedom are restricted. The front impact scenario and its boundary conditions are illustrated in Figure 15. A force of 5370 N is calculated using Equation *(8).*

$$F = m * \frac{dv}{dt} \qquad (8)$$

Where m is the vehicle mass, dv is the velocity difference, $dand\ t$ is the time of the deceleration time. It's assumed that the dt is 0.3 seconds and the vehicle velocity just before impact is 16 km/hr.

Front Impact Loading Results

The results show maximum bending stress of 99.06 MPa occurs as shown in Figure 16 in the secondary longitudinal member at its intersection point with the primary lateral member. Figure 17 shows a maximum absolute torsional moment of 26162 N.mm in the vertical members which produce torsional shear stress of 6.39 MPa as calculated from Equation *(2)*. Moreover, the Normal axial stress of -13.23 MPa is shown in Figure 18 which is less severe than the bending stress. As a result, the factor of safety (F.O.S) of 2.9 is calculated for this scenario from Equation *(6)*. Finally, a maximum deformation of 0.4 mm is generated in the middle of the lower lateral front member as shown in Figure 19.

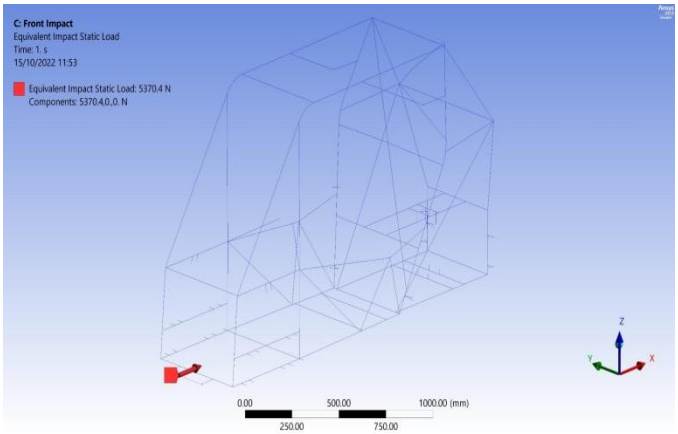

Figure 15 Front-impact loading boundary conditions

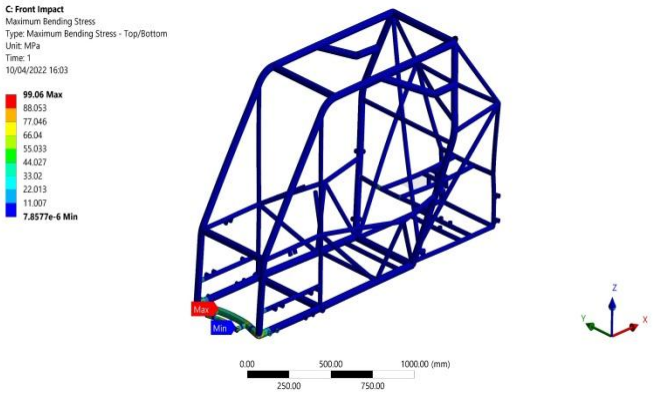

Figure 16 Front-impact bending stress.

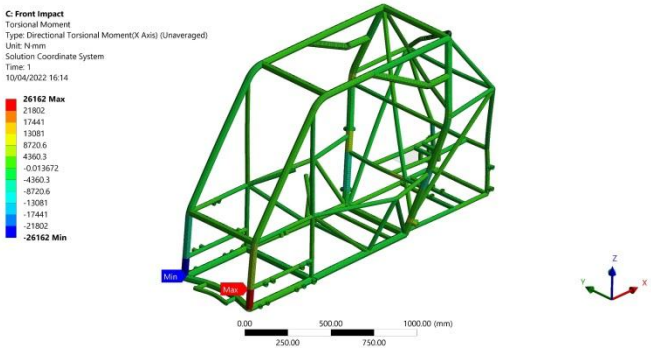

Figure 17 Front-impact torsional moment.

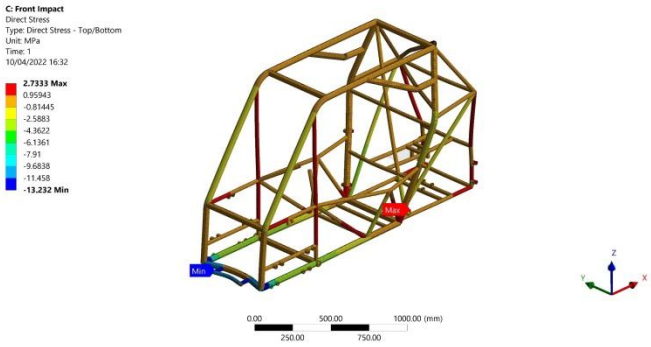

Figure 18 Front-impact axial stress.

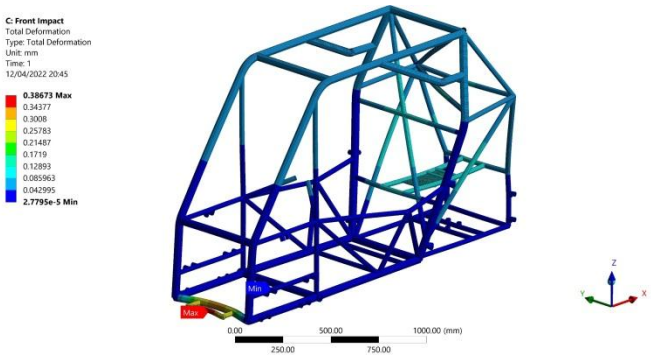

Figure 19 Front-impact total deformation.

Rear Impact Loading Scenario

In this scenario, the vehicle frame is subjected to a rear impact force similar to the exerted force of the front impact scenario. The boundary conditions of the rear impact scenario are shown in Figure 20.

Rear Impact Loading Results

A maximum bending stress of 71.4 MPa is generated at the very rear lateral member subjected to the impact load as shown in Figure 21. Considering this lateral beam, a fixed-fixed ends beam subjected to constant distributed load across its whole length, it is expected to get this result due to the maximum bending moment generated at both fixed ends. Furthermore, the maximum bending stress in the lower lateral member is lower than the upper due to the existence of two longitudinal members supporting the upper member. In addition, due to the deformability of the rear lateral member ends having the maximum bending stress, maximum torsional moments of 38950 N.mm are generated at the vertical members joining that lateral member in opposite directions as shown in Figure 22. This generates maximum torsional shear stress of 17.7 MPa as calculated from Equation *(2)*. Assessing the previous results concerning von-Mises failure criteria, a F.O.S of 4.6 is obtained from Equation *(6)* in this scenario. Finally, a maximum deformation of 0.3 mm occurs in the middle of the rear lateral member as shown in Figure 23.

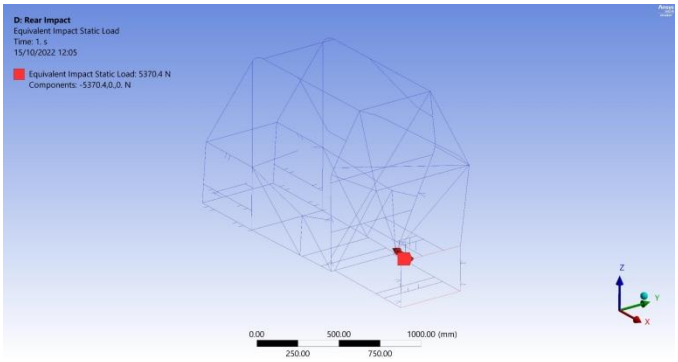

Figure 20 Rear impact loading.

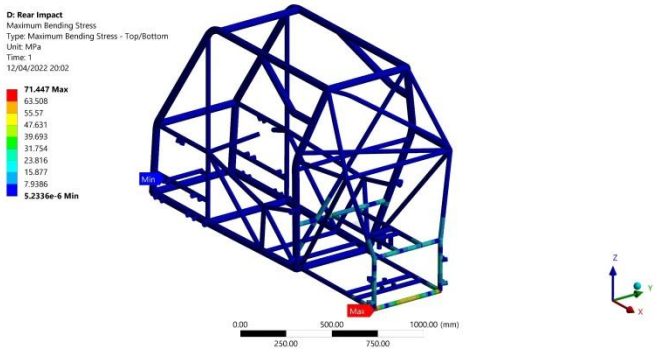

Figure 21 Rear impact bending stress.

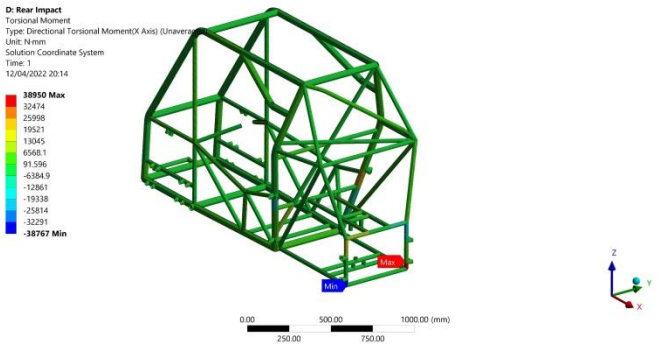

Figure 22 Rear impact torsional moment.

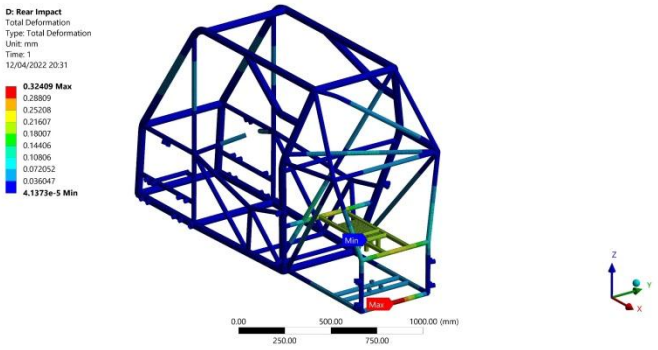

Figure 23 Rear impact total deformation.

Side Impact Loading Scenario

The 3rd scenario involves a side impact equivalent to a static force applied to the longer span of the frame just before the vehicle skidding as shown in the boundary conditions in Figure 24.

Side Impact Loading Results

Maximum bending stress of 120.34 MPa is captured as shown in Figure 25 at the intersection between the vertical and the lateral members. Moreover, a maximum torsional moment of 118480 N.mm is recorded on the lower side frame member as shown in Figure 26 resulting in maximum torsional shear stress of 43.1 MPa which is calculated from Equation *(2)*. Regarding the previous results, a F.O.S of 2.3 can be obtained from Equation *(6)*. Finally, a total deformation of 3.3 mm is recorded in the steering wheel supporting member as shown in Figure 27 which exerts no hazardous effect on the driver.

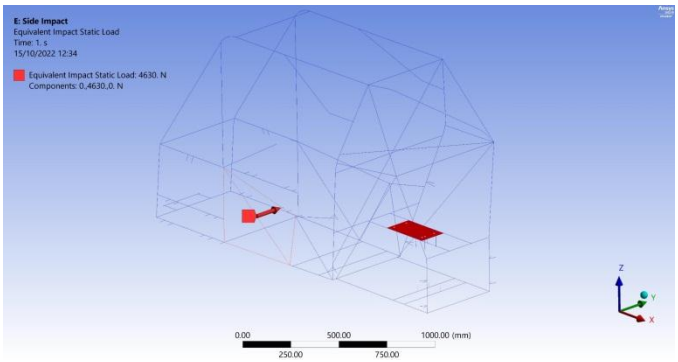

Figure 24 Side impact loading.

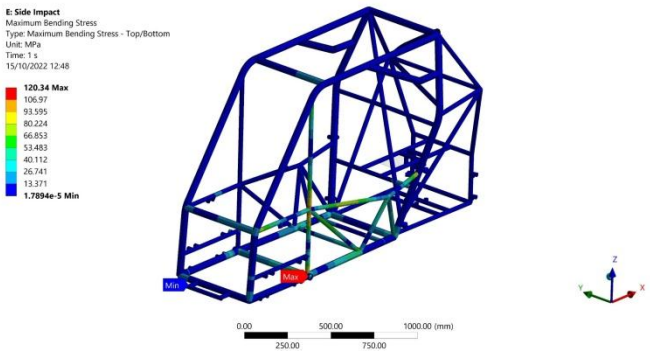

Figure 25 Side impact bending stress.

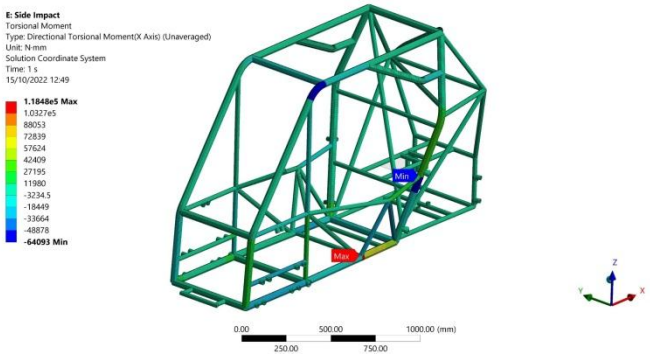

Figure 26 Side impact torsional moment.

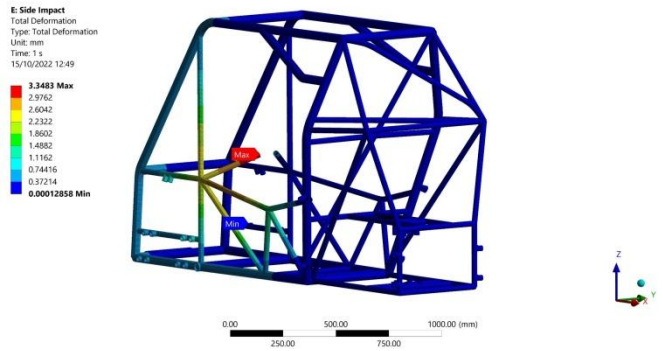

Figure 27 Side impact total deformation.

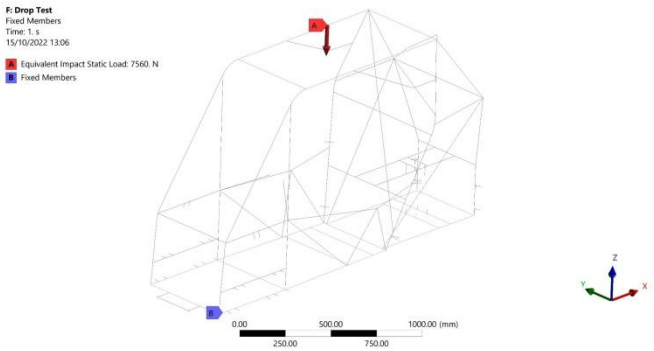

Figure 28 Rollover boundary conditions.

Rollover Scenario

The 4th scenario represents a rollover event, where the vehicle is assumed to have an equivalent impact static load on the top planar four members of the frame, and all the bottom planar members are assumed to be fixed as shown in the boundary conditions in Figure 28. A force of 7560 N is calculated from Equation *(8).* While the velocity dv is calculated with the aid of Equations *(9),* and *(10)* as follows [14]:

$$S = ut + \frac{1}{2}at^2 \qquad (9)$$

$$v = u + at \qquad (10)$$

Where S is the drop distance, u is the initial velocity, a is the vehicle acceleration ($a = g$), t is the drop time, and v is the vehicle final velocity.

Rollover results

Maximum bending stress of 83.6 MPa is captured as shown in Figure 29. Moreover, a maximum torsional moment of 25032 N.mm is recorded occurring in a primary member as shown in Figure 30 which produces maximum torsional shear stress of 9.1 MPa calculated from Equation *(2)*. Additionally, a minimum F.O.S of 3.8 can be calculated for this scenario using Equation *(6).* Finally, a maximum deformation of 1 mm in the negative vertical direction is recorded in the far upper primary members as shown in Figure 31 which has no hazardous effect on the driver and also agrees with the small displacements' assumption.

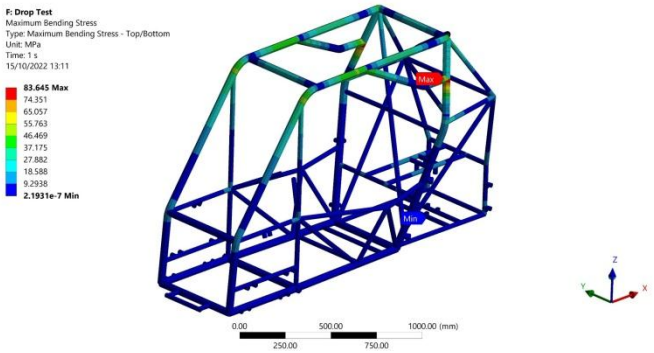

Figure 29 Rollover bending stress.

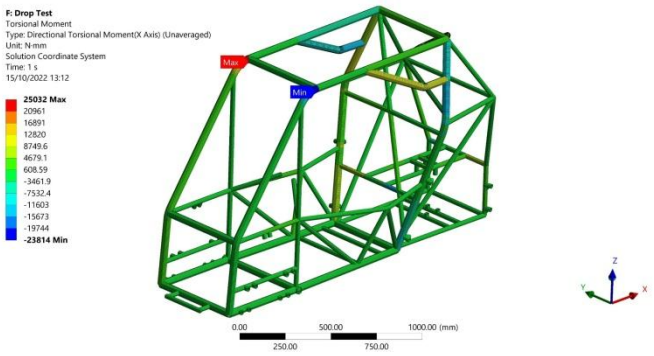

Figure 30 Rollover torsional moment.

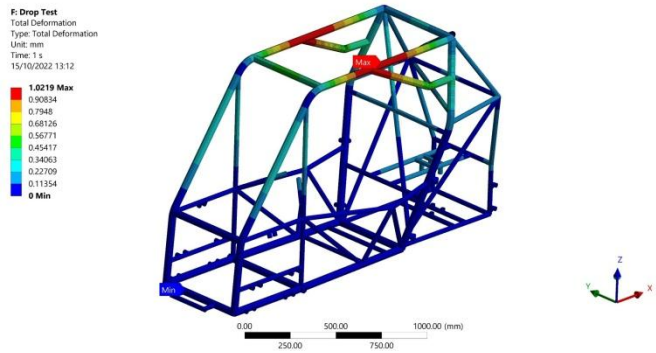

Figure 31 Rollover total deformation.

Torsional stiffness

Torsional stiffness Scenario

This scenario simulates the vehicle's frame behavior when the front wheels are subjected to opposite bumps at the same time. Boundary conditions are illustrated in Figure 32 where the far two cross members are fixed, and two opposite and equal forces are applied at the suspension points in the vehicle frame. Also, the two opposite and equal forces form a couple where the normal distance between the two forces is assumed to be the average distance for those presented in Figure 33 and Figure 34.

Torsional Stiffness Results

Torsional stiffness of 6626.1 $N.m/degree$ is calculated from Equation *(11)* where the angle θ is the twisting angle due to maximum and minimum deformation as observed from Figure 36. The torsional stiffness formula is expressed as [15]

$$Torsional\ Stiffness = \frac{Force * L_{avg}}{\theta} \qquad (11)$$

Where L_{avg} is the average distance between upper and lower suspension points.

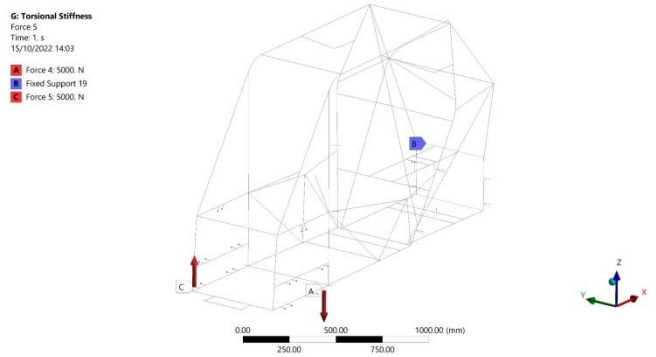

Figure 32 Torsional stiffness boundary conditions

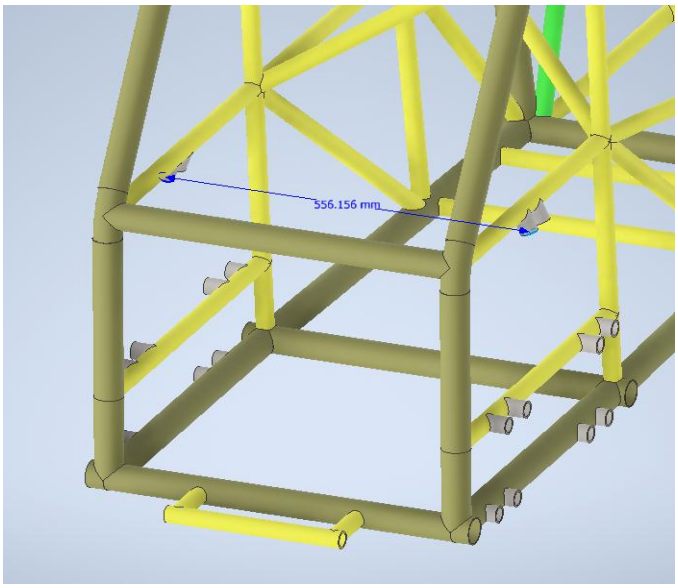

Figure 33 Front upper axle center to center distance

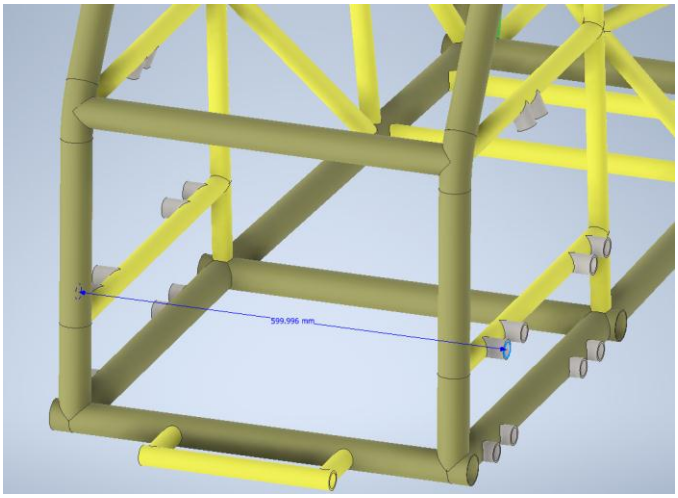

Figure 34 Front axle lower center-to-center distance

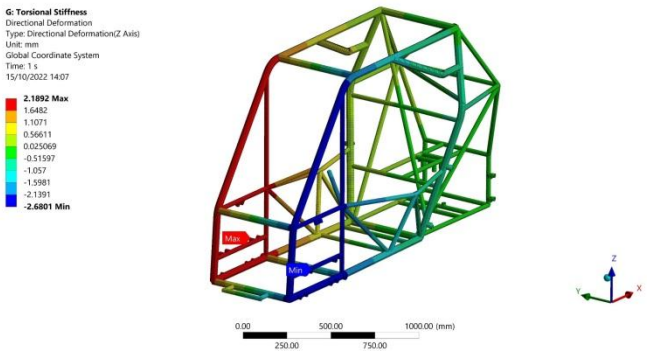

Figure 35 Torsional stiffness directional (Z-axis) deformation

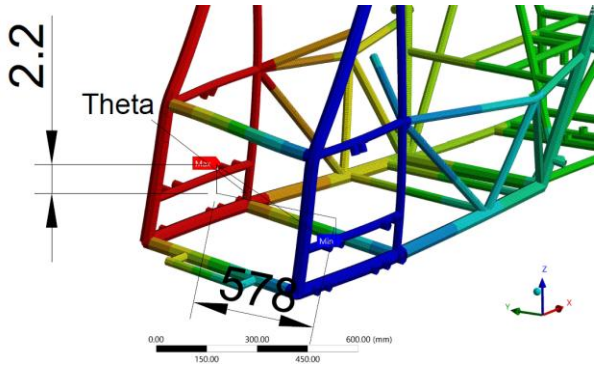

Figure 36 Torsional stiffness results

Conclusions

This research focuses on the design and validation of the SAE BAJA space frame which is modeled and analyzed using FEA. The design process includes three different stages. In the 1st stage, selection of the frame members cross sections and the material is selected considering aspects of the material availability and the competition rules. While in the 2nd stage, the frame CAD model is constructed in SolidWorks software. The final stage includes testing the vehicle frame using many simulation scenarios that the off-road vehicle design could face in the competition environment. These scenarios consider the vehicle frame stresses due to longitudinal and lateral load transfer, road grade, and rotational acceleration. Also, vehicle impact and rollover scenarios are analyzed as well as the vehicle torsional stiffness test. The proposed vehicle frame design fulfils all aspects of the safety requirements with an acceptable factor of safety values according to the simulation scenarios.

References

[1] "Collegiate Design Series Baja SAE ® Rules." [Online]. Available: https://bajasae.pyrotectstore.com/.

[2] D. Raina, R. Dev Gupta, and R. Kumar Phanden, "Design and Development for Roll Cage of All-Terrain Vehicle," *International Journal For Technological Research In Engineering (IJTRE)*, vol. 2, no. 7, 2015.

[3] A. T. Owens, M. D. Jarmulowicz, and P. Jones, "Structural Considerations of a Baja SAE Frame."

[4] S. Fu *et al.*, "Optimal Design of the Frame of Baja Racing Car for College Students," in *Lecture Notes in Electrical Engineering*, 2022, vol. 769, pp. 293–310. doi: 10.1007/978-981-16-2090-4_17.

[5] S. Krishna, A. Shetye, and P. Mallapur, "Design and Analysis of Chassis for SAE BAJA Vehicle." [Online]. Available: www.iosrjen.org

[6] A. S. Shridhar, A. Tukkar, A. Vernekar, V. Badderu, A. Y. Patil, and B. B. Kottursheettar, "Modeling and Analysis of ATV Roll Cage," 2020, pp. 281–292. doi: 10.1007/978-981-13-8468-4_21.

[7] Y. Chandra, "Design, Analysis and Optimization of a BAJA-SAE Frame," *International Journal of Science and Research*, 2018, doi: 10.21275/SR20208233756.

[8] A. Burke and J. Carlos Miranda, "Minibaja Frame Design using Topological Optimization and Impact Testing," 2006.

[9] N. Noorbhasha and B. J. O'Toole, "Static Analysis on a Roll Cage Frame for an Off-Road Vehicle," in *SAE Technical Papers*, Mar. 2017, vol. 2017-March, no. March. doi: 10.4271/2017-01-1299.

[10] "Practical Aspects of Finite Element Simulation A Study Guide Academic Program," 2015.

[11] R. G. Budynas and J. Keith Nisbett, "Shigley's Mecha nical Engineering Design."

[12] S. Javanbakht, "Error calculation for beginners an example-oriented introduction for students of the TUHH." [Online]. Available: https://www.researchgate.net/publication/283292479

[13] J. Y. (Jo Y. Wong, *Theory of ground vehicles*. John Wiley, 2001.

[14] *Brake Design and Safety*. 1999. doi: 10.4271/9780768027105.

[15] D. Krzikalla, J. Mesicek, J. Petru, A. Sliva, and J. Smiraus, "Analysis of Torsional Stiffness of the Frame of a Formula Student Vehicle," *J Appl Mech Eng*, vol. 08, no. 01, 2019, doi: 10.35248/2168-9873.19.8.315.

Nomenclature

a - vehicle acceleration.

dt - deceleration time.

dv - velocity difference.

g - gravitational acceleration.

h - vehicle C.G height from the ground.

I - second moment of inertia.

J - polar moment of area.

L - vehicle wheelbase.

L_{avg} - average distance between upper and lower suspension points.

l_1 - Distance between the vehicle's front axle and its CG.

l_2 - Distance between the vehicle's rear axle and its CG.

M - bending moment.

m - vehicle mass.

S - drop distance.

T - torque.

t - drop time.

u - vehicle initial velocity.

v - vehicle final velocity.

W - vehicle weight.

W_f - vehicle load on the front axle.

W_r - vehicle load on the rear axle.

x - analytical value.

y - max. distance from the neutral axis.

Δx - difference between the analytical value and the value of every mesh.

θ - twisting angle.

θ_s - road inclination angle.

σ - bending stress.

$\sigma_{Von-Mises}$ - von-mises stress.

σ_{yield} - yield strength.

τ - shear stress.

Contact Information

Poula Magdy Kamel

Teaching Assistant, Faculty of Engineering, Mataria, Helwan University

Poula.m.kamel@m-eng.helwan.edu.eg